

Springer Series in Materials Science

Editors: U. Gonser · A. Meoradian · K. A. Müller · M. B. Panish · H. Sakaki
Managing Editor: H. K. V. Loitsch

- Volume 1 **Chemical Processing with Lasers**
By D. Bäuerle
- Volume 2 **Laser-Beam Interactions with Materials**
Physical Principles and Applications
By M. von Allmen
- Volume 3 **Laser Processing of Thin Films and Microstructures**
Oxidation, Deposition and Etching of Insulators
By I. W. Boyd
- Volume 4 **Microclusters**
Editors: S. Sugano, Y. Nishina, and S. Ohnishi
- Volume 5 **Graphite Fibers and Filaments**
By M. S. Dresselhaus, G. Dresselhaus,
K. Sugihara, I. L. Spain, and H. A. Goldberg
- Volume 6 **Elemental and Molecular Clusters**
Editors: G. Benedek, T. P. Martin, and G. Pacchioni
- Volume 7 **Molecular Beam Epitaxy** Fundamentals and Current Status
By M. A. Herman and H. Sitter
- Volume 8 **Physical Chemistry of, in and on Silicon**
By G. F. Cerofolini and L. Meda
- Volume 9 **Tritium and Helium-3 in Metals**
By R. Lässer
- Volume 10 **Computer Simulation of Ion – Solid Interactions**
By W. Eckstein
- Volume 11 **Mechanisms of High Temperature Superconductivity**
Editors: H. Kamimura and A. Oshiyama
- Volume 12 **Laser Technology in Microelectronics**
Editors: S. Metev and V. P. Veiko
- Volume 13 **Semiconductor Silicon**
Materials Science and Technology
Editors: G. C. Harbeke and M. J. Schulz

H. Kamimura A. Oshiyama (Eds.)

Mechanisms of High Temperature Superconductivity

Proceedings of the 2nd NEC Symposium,
Hakone, Japan, October 24–27, 1988

With 203 Figures

Springer-Verlag Berlin Heidelberg New York
London Paris Tokyo

Cu distance, the magnetic susceptibility does not exhibit the negative temperature coefficient. Instead, the temperature dependence is characterized by the Curie-like behavior.

IV. ACKNOWLEDGMENT

The authors would like to thank M. Ueta, T. Ido, S. Ishibashi for their help in the experiments. This work was supported by a grant-in-aid of Scientific Research of the Special Project Research on the High Temperature oxide Superconductors from the Ministry of Education, Science and Culture.

References

1. K. Kitazawa, H. Takagi, K. Kishio, T. Hasegawa, S. Uchida, S. Tajima, S. Tanaka and K. Fueki, for a comprehensive review on the experimental works, see also other articles in this volume.
2. J. B. Torrance, Y. Tokura, A. I. Nazzal, A. Bezinge, T. C. Huang and S. S. P. Parkin: *Phys. Rev. Lett.* **61**, 1127 (1988).
3. H. Takagi et al. to be submitted.
4. A. I. Nazzal et al.: *Physica* **135-156C**, 1367 (1988).
5. J. Gopalakrishnan, G. Colmann and B. Reuter: *J. Solid State Chem.* **22**, 145 (1977).
6. A. R. Moodenbaugh, Y. Xu, M. Suenaga, T. J. Folkerts and R. N. Shelton: *Phys. Rev.* **B38**, 4596 (1988).
7. S. Uchida, H. Takagi, H. Ishii, H. Eisaki, T. Yabe, S. Tajima and S. Tanaka: *Jpn. J. Appl. Phys.* **26**, 440 (1987).
8. N. P. Ong, Z. Z. Wang, J. Clayhold, J. M. Tarascon, L. H. Green and W. R. Mackinnon: *Phys. Rev.* **B35**, 8807 (1987).
9. H. Fukuyama and Y. Hasegawa: *Physica* **148B**, 204 (1987).
10. S. W. Tozer, A. W. Kleinsasser, T. Penny, D. Kaiser and F. Holtzberg: *Phys. Rev. Lett.* **59**, 1768 (1987).
11. Y. Iye, T. Tamegai, H. Takeya and H. Takei: *Jpn. J. Appl. Phys.* **26**, L1057 (1987).
12. M. Suzuki: *Phys. Rev.* **B**, Submitted.
13. Y. Iye, T. Tamegai, T. Sakakibara, T. Goto, N. Miura, H. Takeya and H. Takagi: *Physica* **C153-155**, 26 (1988).
14. T. Fujita, Y. Aoki, Y. Maeno, J. Sakurai, H. Fukuba and H. Fujii: *Jpn. J. Appl. Phys.* **26**, L368 (1987).
15. R. J. Birgeneau, D. R. Gabbe, H. P. Jenssen, M. A. Kastner, P. J. Picoe, T. R. Thurston, G. Shirane, Y. Endoh, M. Satoh, K. Yamada, Y. Hidaka, M. Oda, Y. Enomoto, M. Suzuki and T. Murakami: *Phys Rev.* **B37**, 7443 (1988).
16. D. C. Johnston, S. K. Sinha, A. J. Jacobson and J. M. Newsam: *Physica* **C153-155**, 572 (1988).
17. H. A. Algra, L. J. de Jongh and R. L. Carlin: *Physica* **93B**, 24 (1978).
18. R. J. Birgeneau, M. A. Kastner, A. Aharony, G. Shirane and Y. Endoh: *Physica* **C153-155**, 515 (1988).
19. R. J. Birgeneau, M. A. Kastner and A. Aharony: Preprint.

Anisotropic Transport in Y-Ba-Cu-O and Bi-Sr-Ca-Cu-O

A. Zettl, A. Behrooz, G. Briceño, W. N. Creager, M. F. Crommie, S. Hoën, and P. Pinsukanjana

Department of Physics, University of California at Berkeley, and
Materials and Chemical Sciences Division, Lawrence Berkeley Laboratory,
Berkeley, California, CA 94720, USA

The anisotropic normal state transport properties of the superconducting oxides Y-Ba-Cu-O and Bi-Sr-Ca-Cu-O are investigated by dc resistivity, thermoelectric power, high frequency conductivity, and uniaxial stress effects in single crystals. We also explore the superconducting state by measurements of T_c under c-axis stress, and oxygen isotope substitution. Energy gap structure is investigated by break junction single-crystal tunneling.

1. INTRODUCTION

The new classes of oxide superconductors based on Cu-O₂ sheets have unusual superconducting and normal state properties. The sheet structure gives rise to quasi-two-dimensional electronic structure with large anisotropy in the normal state. The low dimensionality has been exploited in numerous models of high- T_c superconductivity. The unusually high transition temperatures, together with the observed reduced isotope effect, suggest a new electron pairing mechanism. A good understanding of the superconducting properties of a material necessitates a good understanding of the normal state properties.

We here explore anisotropy in the normal states, and to a lesser degree in the superconducting states, of the oxide superconductors Y-Ba-Cu-O and Bi-Sr-Ca-Cu-O. We find that the electronic conduction in the normal state is not well described by conventional mechanisms, in particular in the direction perpendicular to the Cu-O₂ planes. Our findings place restrictions on the type of transport possible in the normal state, and indirectly on the superconductivity mechanism.

2. ANISOTROPIC TRANSPORT IN YBa₂Cu₃O_{7-δ}

2.1 Resistivity and Thermoelectric Power

As first demonstrated by TOZER et al [1], the resistivity tensor in YBa₂Cu₃O₇ single crystals suggests a substantial temperature-dependent anisotropy. In fact, for many crystals, the c-axis resistivity appears "semiconductor-like" while the a-b plane resistivity appears metallic. For some crystals, on the other hand, the "upturn" in the c-axis resistivity starts only very close to T_c [2]. The difference may be a combination of impurities (including oxygen vacancy) and degree of twinning

in the a-b plane. For any crystal, the upturn is easily enhanced by depleting the oxygen content, i.e. increasing δ .

For a typical high purity crystal with full oxygen content, the c-axis resistivity at room temperature is of order 10-20 m Ω cm. In the tight-binding approximation, the electronic mean free path is given by [3]

$$\lambda = v_F \tau = \hbar v_F / 4ne^2 a \quad (1)$$

where n is the carrier density, v is the conductivity in the direction in question, and a is the lattice constant in the direction in question. The carrier concentration in $\text{YBa}_2\text{Cu}_3\text{O}_y$ is of order $10^{22}/\text{cm}^3$. Eq. (1) then gives for the c-axis mean free path $\lambda = 10^{-5} \text{Å}$, clearly an unphysical value. This immediately suggests that band transport is inappropriate to $\text{YBa}_2\text{Cu}_3\text{O}_y$, at least along the c-axis. In sections below we test various predictions of band theory for the c-axis conduction, and consistently find discrepancies.

Fig. 1 shows [2] the normalized c-axis resistivity for $\text{YBa}_2\text{Cu}_3\text{O}_7$ corresponding to three different oxygen concentrations, $\delta = 0, 0.5, \text{ and } 0.7$. We respectively label these samples pristine oxygenated (PO), oxygen deficient (OD), and very oxygen deficient (VOD). The VOD state is not superconducting at any temperature. It is tempting to describe the temperature dependence as "semiconductor like". Fig. 2a shows the data of Fig. 1 plotted as $\log(\rho)$ vs $1/T$. Only at high temperatures does the conductance appear thermally activated, with corresponding activation energies $E_a = 2.4 \text{meV}, 4 \text{meV}, \text{ and } 450 \text{meV}$ for PO, OD, and VOD samples, respectively. At low temperatures, the data curve away from exponential behavior in a manner similar to low-dimensional disordered metals, where carriers become localized with decreasing temperature. In a regime of strong localization, one expects for a three dimensional system a temperature dependence

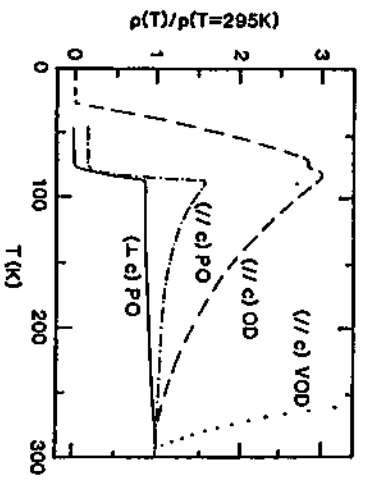


Figure 1. Normalized c-axis resistivity of $\text{YBa}_2\text{Cu}_3\text{O}_y$ for different oxygen contents. The a-b plane resistivity is also shown for a fully oxygenated sample.

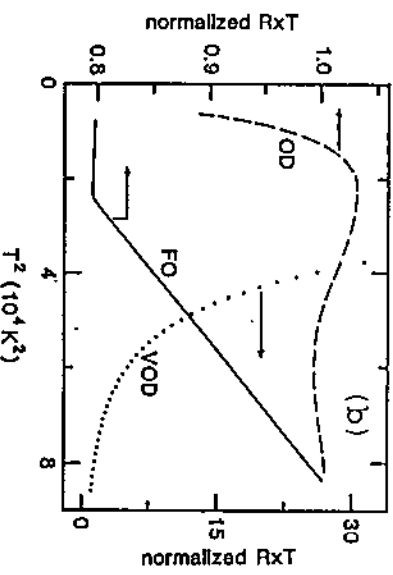
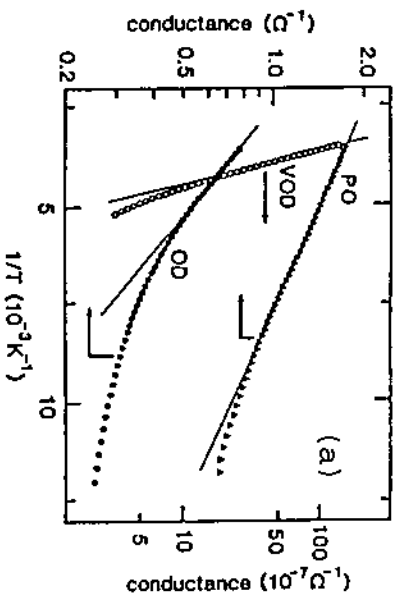


Figure 2. a) Fits to activated "semiconductor-like" conductivity for c-axis conductance in $\text{YBa}_2\text{Cu}_3\text{O}_y$. Data for three different oxygen contents are shown. The data are activated only at high temperatures, where the activation energy increases with decreasing oxygen content. b) Fits to the Anderson-Zou hole soliton c-axis tunneling formula, Eq. (4). The $\text{YBa}_2\text{Cu}_3\text{O}_y$ data fit the formula only for full oxygen content and only at high temperatures.

$$\sigma = \sigma_0 \exp[-(T_0/T)^{1/4}] \quad (2)$$

while in the regime of weak localization one has

$$\sigma = \sigma_0 + 2ne^2 \tau^3 / 2 \hbar m^3 v \quad (3)$$

The data of Fig. 1 fits neither Eq. (2) or (3), nor their analogs for two or one dimensional systems. We also note that we have observed no unusual magnetoresistance effects in the c-axis conduction, again giving evidence against standard localization behavior.

ANDERSSON and ZOU[4] have suggested that if the normal state of $\text{YBa}_2\text{Cu}_3\text{O}_7$ is described by a resonating valence bond (RVB) state, the c-axis conduction is dominated by tunneling between planes of hole solitons with an expected temperature $1/T$ dependence, i.e.

$$\rho_c = A/T + BT \quad (4)$$

where the term linear in T accounts for experimental "contamination" from a-b plane conduction. To test Eq. (4), one plots $\rho_c T$ vs T^2 , as was originally done by HAGEN et al[5]. Fig. 2b shows our c-axis resistivity plotted in this way to test Eq. (4). It is apparent that a reasonable (linear) fit occurs only for high oxygen content, and even then only over a restricted temperature range.

A general empirical expression has been suggested[6] for the c-axis resistivity in $\text{YBa}_2\text{Cu}_3\text{O}_7$,

$$\rho_c = T^{\alpha} \exp\{E_g/K_B T\}, \quad (5)$$

where α is a constant between 0.5 and 1.0 and E_g represents a reduced or effective gap for activated charge transport. Eq. (5) appears to fit well the c-axis conductivity for different $\text{YBa}_2\text{Cu}_3\text{O}_7$ crystals with $E_g \approx 25\text{meV}$. This is shown in Fig. 3, where $\ln[\rho_c/T^{\alpha}]$ is plotted versus $1/T$, using data from two different research groups. One physical interpretation[6] of Eq. (5) is that the exponential term arises from activated behavior similar to the conductivity in amorphous semiconductors, while the T^{α} term comes from the temperature dependence of the mobility, and hence the scattering time τ . Possible sources of the temperature number and the average carrier velocity.

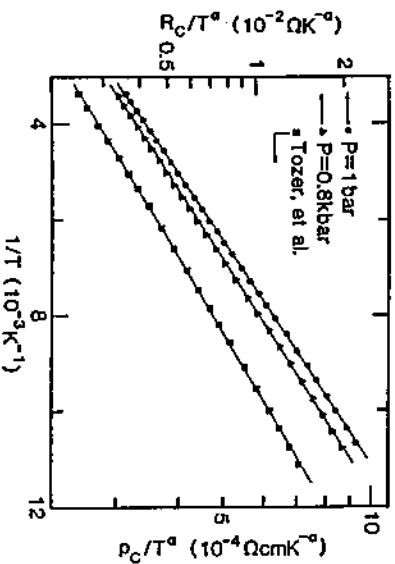


Figure 3. Fits of c-axis conductivity in $\text{YBa}_2\text{Cu}_3\text{O}_7$ to Eq. (5), with the specimen at ambient pressure and under c-axis pressure. Fits to data of ref. 1 are also shown.

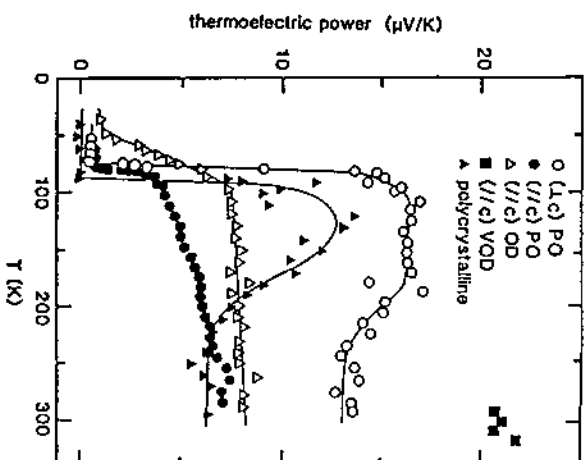


Figure 4. Thermoelectric power for $\text{YBa}_2\text{Cu}_3\text{O}_y$ for different directions in the crystal and for different oxygen contents. The polycrystalline result for full oxygen content is also shown.

Another transport coefficient complementary to the resistivity is the thermoelectric power (TEP). For a metal one expects a TEP linear in temperature, neglecting phonon drag effects. For a semiconductor with gap E_g , the TEP is proportional to $E_g/K_B T$. In the superconducting state, the superconducting electrons to first order short out any thermally induced EMF, hence the TEP is zero. Fig. 4 shows[6] the TEP for different crystal directions and oxygen contents of $\text{YBa}_2\text{Cu}_3\text{O}_7$. Also shown is the TEP for a polycrystalline sample. The a-b plane TEP is not linear in T (and is similar to the polycrystalline result), in contrast to what might be expected from the a-b plane metallic resistivity. The c-axis TEP is linear in T , and hence not of the semiconductor form.

ALLEN et al[7] have investigated the phonon-induced resistivity ρ_{ph} , Hall coefficient R_H^{ph} , and TEP S_{ph} for $\text{YBa}_2\text{Cu}_3\text{O}_y$ based on band structure calculations using a variational solution of the Boltzman transport equations. Some of the data in Fig. 4 are consistent with these predictions, but discrepancies exist. For example, the measured TEP is positive (holelike) both in the a-b plane and along the c-axis, while ALLEN et al predict that S_{xx} and S_{yy} will be negative, and the sign of S_{zz} is dependent on the choice of $\tau(\epsilon)$ (x and y are in the a-b plane, z is parallel to the c-axis).

2.2 High-frequency ac Conductivity

The electrical conductivity of metals and semiconductors is frequency dependent. For a metal the characteristic energy for frequency dependent conductivity is ω^{-1} (or $\omega \sim 10^{14}$ Hz), while for a semiconductor it is $\hbar\omega/2\pi \sim 2E_g$. From Eq. (5) where the effective "gap" energy is ~ 25 meV, we might expect frequency dependent conductivity near 6×10^{12} Hz for the c-axis conduction. On the other hand, several non-band transport mechanisms (including localization and variable range hopping) give frequency dependent conductivities at much lower characteristic energies, often with power law dependences such as

$$\sigma(\omega) \sim \omega^5.$$

(6)

TESTARDI et al [8] have reported unusually large dielectric constants in thermally quenched (oxygen deficient) polycrystalline $YBa_2Cu_3O_{7-x}$ at very low (audio) frequencies, while REAGOR et al [9] report a strong frequency dependent conductivity in single crystal (nonsuperconducting) Eu_2CuO_4 in the microwave regime.

We have investigated the frequency dependent conductivity of $YBa_2Cu_3O_{7-x}$ single crystal specimens with different oxygen content in the frequency range 5 Hz to 1 GHz. Figs. 5a,b show the dc and ac (1 GHz) conductivities from room temperature to below T_c . For neither the a-b plane direction nor the c-axis direction do we observe any unusual frequency dependences. This is true regardless of the oxygen content, and suggests that the effective activation energy associated with Eq. (5) is a meaningful energy scale. It also suggests that the unusual dielectric (capacitance) effect observed by TESTARDI et al is not an intrinsic effect, but is most probably due to capacitances formed at grain boundaries in polycrystalline specimens.

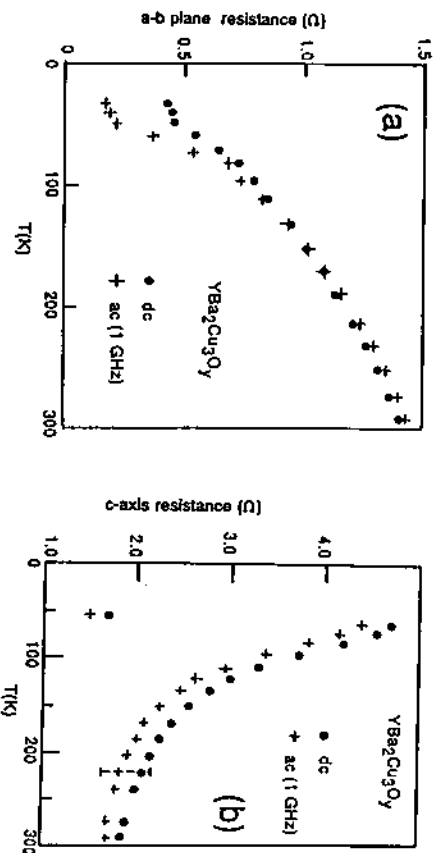


Figure 5. dc and ac (1GHz) resistance of $YBa_2Cu_3O_7$ (slightly oxygen deficient) for a) a-b plane, and b) c-axis.

2.3 Role of Interplane Coupling and the Superconductivity Mechanism

The above results imply that conventional band transport does not describe the c-axis conduction in $YBa_2Cu_3O_7$. The important question thus arises, is the superconductivity at lower temperature driven by a novel mechanism? One of the most obvious concerns is the role of the Cu-O₂ planes, i.e. the dimensionality of the system. A number of models [10] take advantage of the special properties of a two dimensional system (such as density of states anomalies) to account for the high T_c 's (and other unusual features such as the reduced isotope effect).

We have investigated the role of interplane coupling in $YBa_2Cu_3O_7$ by directly changing the interplane separation (through externally applied uniaxial stress) and measuring the effect on the resistivity tensor and T_c [6]. Fig. 6 shows the experimental configuration. c-axis stress (or pressure) is applied to the single crystal using a steel-sample-steel sandwich. An epoxy film electrically insulates the a-b plane surfaces of the crystal from the steel discs. The a-b plane and c-axis resistivities are determined by four-probe wire contact methods. For c-axis pressures up to 1 kbar, there is no observed effect on the magnitude or temperature dependence of the a-b plane resistivity. The c-axis resistivity, on the other hand, is dramatically changed, as demonstrated in Fig. 7. The general trend is that increasing c-axis pressure (i.e. decreasing interplane separation) leads to a decrease in $\rho_c(T)$. The inset to Fig. 7 shows that the functional form of the $\rho_c(T)$ curves is altered by pressure: increasing pressure tends to make the

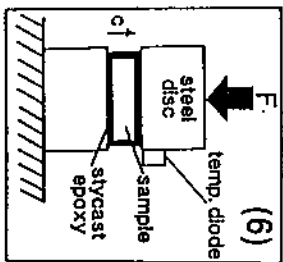


Figure 6

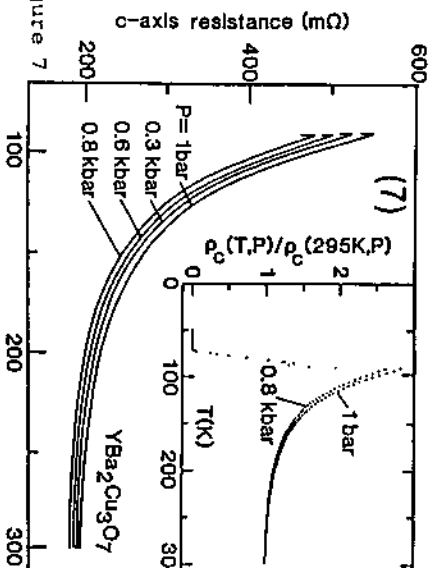


Figure 7

Figure 6. Pressure cell for applying uniaxial stress to single crystals.

Figure 7. c-axis resistance vs T for selected c-axis pressures in $YBa_2Cu_3O_7$. The inset shows normalized resistivity data for the two extreme pressures.

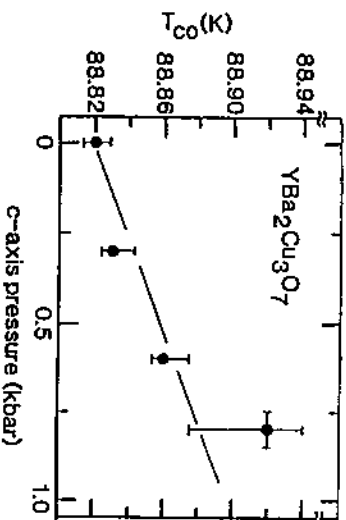


Figure 8. Superconducting onset temperature versus c-axis pressure in $\text{YBa}_2\text{Cu}_3\text{O}_7$. Decreasing interplanar spacing increases T_c .

c-axis resistivity more metallic. The most direct interpretation of this effect is that c-axis stress increases the matrix element t_{\perp} for interplanar charge transfer. From considerations of non-band anisotropic conduction [11], one may crudely approximate

$$\rho_c/\rho_{a-b} \approx (t_{\perp}/t_{\parallel})^2. \quad (7)$$

The data of Fig. 7 indicate $d \ln t_{\perp} / dP = +0.08/\text{kbar}$ at 95K.

How does T_c depend (if at all) on t_{\perp} ? Fig. 8 shows that T_c increases smoothly as the c-axis stress is increased. In other words, T_c increases as the electronic coupling between the planes is increased. With the measured $dT_c/dP = 0.08\text{K/kbar}$, we find $dT_c/d \ln t_{\perp} = 1$. This result rules out strictly two dimensional superconductivity mechanisms.

2.4 Filamentary Superconductivity and the Isotope Effect

In a homogeneous single-crystal superconductor, the transition temperature is usually well-defined. At T_c the resistance abruptly drops to zero and the specimen becomes (in low applied field) a perfect diamagnet. Sample inhomogeneities can lead to a smeared transition. Conductivity measurements always measure the path of least resistance, and hence are not always a good indicator of "bulk superconductivity"; for this the dc magnetization is in general a better probe.

Recent measurements [12] have indicated that in freshly prepared high- T_c polycrystalline specimens, T_c determined resistively is as much as 2K higher than T_c determined magnetically. The latter measurement determines the bulk transition temperature for the superconducting grains. The discrepancy is evidence for filamentary superconductivity in polycrystalline samples. The fact that the filamentary T_c is higher than the bulk T_c suggests that a small part of the sample (perhaps near the grain boundaries) is actually a different

material, with a volume fraction too small for x-ray detection. Alternatively, the potentially novel superconductivity mechanism may be sensitive to sample geometry and boundary effects. In this case, the filamentary superconductivity occurs in pure $\text{YBa}_2\text{Cu}_3\text{O}_7$ but only where it is truncated geometrically. We have found [12] that filamentary superconductivity in $\text{YBa}_2\text{Cu}_3\text{O}_7$ is time dependent and disappears after several months. This makes the first suggestion more probable, i.e. that the filamentary superconductivity corresponds to an unstable phase which degrades with a time constant of several months.

We have examined if the superconductivity mechanism for filamentary superconductivity is the same as for the bulk material. Isotope substitutions on the oxygen sites were performed using polycrystalline specimens of $\text{YBa}_2\text{Cu}_3\text{O}_7$. With up to 95% of the ^{16}O replaced with the ^{18}O isotope, T_c is found to be decreased for both filamentary and bulk superconductivity. The relative decrease in T_c for filamentary superconductivity was slightly but not significantly greater. Assuming the relation

$$T_c - M \propto \alpha \quad (8)$$

where M is the oxygen mass, we find [12] for filamentary superconductivity $\alpha = 0.028 \pm 0.003$ and for bulk superconductivity $\alpha = 0.019 \pm 0.004$. These values are the extrapolated values, appropriate to 100% isotopic substitution. They are much smaller than the standard BCS prediction $\alpha = 0.5$, and are inconsistent with three dimensional phonon-mediated pairing in general [12,13]. It seems appropriate to at least consider three dimensional theory in light of the sensitivity of T_c to interplanar coupling and the relatively high transition temperatures of the isotropic oxide superconductors Ba-K-Bi-O [14]. The calculation has not been performed assuming a dimensionally restricted phonon interaction.

3. ANISOTROPIC TRANSPORT IN Bi-Sr-Ca-Cu-O

We have investigated two distinct Bi-Sr-Ca-Cu-O single crystal structures. The first is $\text{Bi}_2\text{Sr}_2\text{CaCu}_2\text{O}_8$, a relatively well-known compound with $T_c = 88\text{K}$. This material shares common features with $\text{YBa}_2\text{Cu}_3\text{O}_7$. The usual crystals are mica-like platelets with the c-axis perpendicular to the untwinned plate surface. It is relatively easy to cleave the crystals in the a-b plane. We have also synthesized a new Bi-Sr-Ca-Cu-O structure [15]. The crystals grow with a long thin needle morphology, with the c-axis along the needle axis. The structure at room temperature, determined from single crystal x-ray analysis, is orthorhombic, with unit cell dimensions $a = 13.12\text{\AA}$, $b = 11.44\text{\AA}$, $c = 7.469\text{\AA}$. The c-axis dimension is less certain because of an incommensurate superstructure present. The nominal composition of the needle-like crystals was determined from SEM analysis to be approximately $\text{Bi}_0.1\text{Sr}_{2.2}\text{Ca}_{1.1}\text{Cu}_6\text{O}_y$, i.e. compared to standard Bi-Sr-Ca-Cu-O compounds, this material is extremely Bi poor and Cu rich. T_c onset is approximately 90K. Magnetization studies indicate bulk superconductivity below T_c .

3.1 Resistivity and Thermoelectric Power

Fig. 9a shows the resistivity of single crystal $\text{Bi}_2\text{Sr}_2\text{CaCu}_2\text{O}_8$ using the standard Montgomery method. The resistances R_1 and R_2 have the usual meaning, and reflect (but do not equal) the c-axis and a-b plane resistivities, respectively. The resistivity tensor is highly anisotropic and again the c-axis conduction is not metallic. The c-axis resistance of a $\text{Bi}_{0.1}\text{Sr}_{1.9}\text{Ca}_{1.1}\text{Cu}_{6.5}\text{O}_y$ needle is shown in Fig. 9b. There is a dramatic upturn in the resistance with decreasing temperature above T_c . We have attempted to fit the c-axis conduction of the needle crystals to formulas described above for $\text{YBa}_2\text{Cu}_3\text{O}_7$. Figs. 10a-c show respectively fits to simple activated behavior (semiconductor-like), Eq. (4)

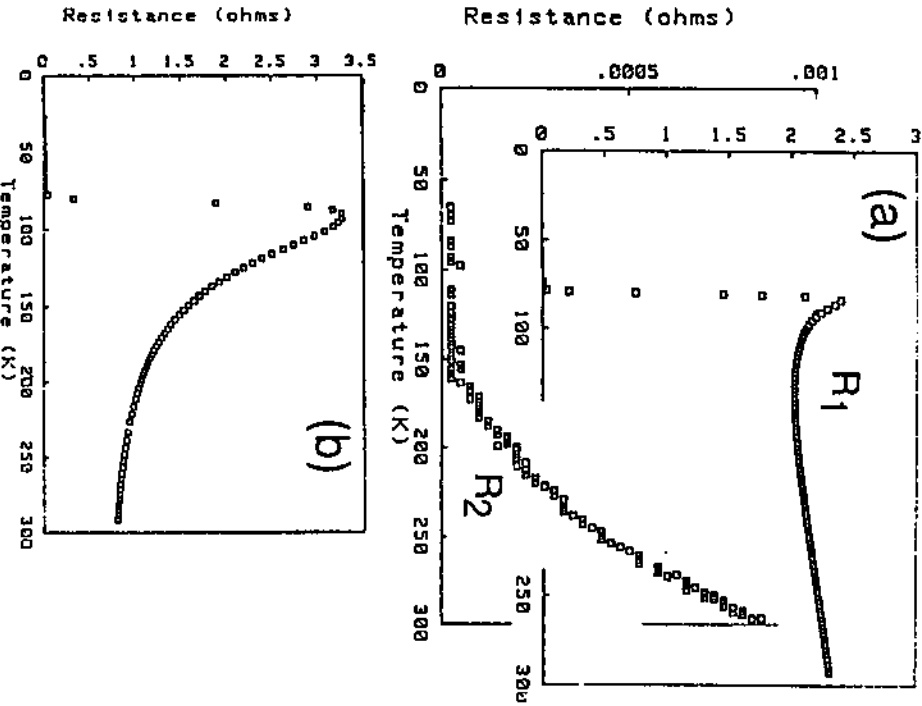


Figure 9. a) anisotropic resistances R_1 and R_2 from Montgomery method for $\text{Bi}_2\text{Sr}_2\text{CaCu}_2\text{O}_8$. b) c-axis resistance of $\text{Bi}_{0.1}\text{Sr}_{2.2}\text{Ca}_{1.1}\text{Cu}_{6.5}\text{O}_y$ needle crystals.

258

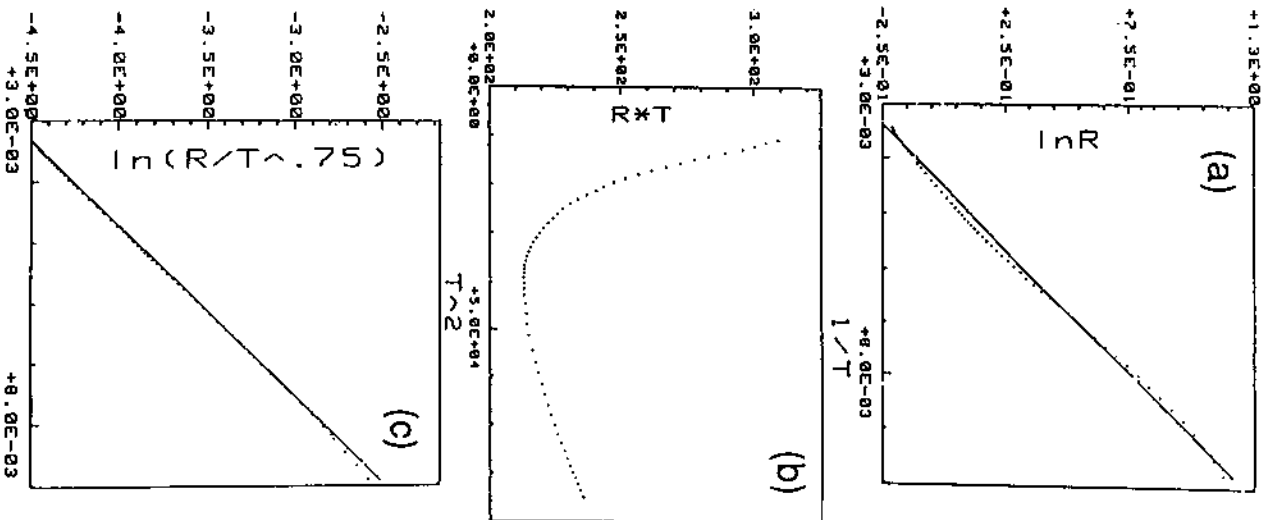


Figure 10. Fits of c-axis resistance of $\text{Bi}_{0.1}\text{Sr}_{2.2}\text{Ca}_{1.1}\text{Cu}_{6.5}\text{O}_y$ to a) activated semiconductor formula, b) RVB tunneling (Eq. 4), and c) empirical formula Eq. (5) with $\alpha=0.75$; $\epsilon_g=32\text{meV}$.

259

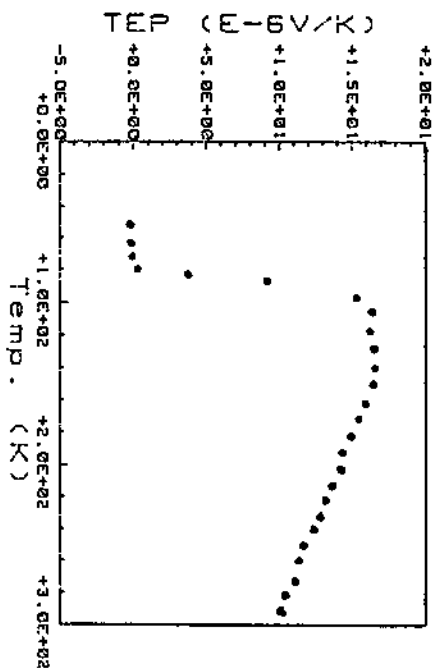


Figure 11. Thermoelectric power of $\text{Bi}_2\text{Sr}_2\text{CaCu}_2\text{O}_8$ in the a-b plane.

(appropriate to the RVB state), and the empirical expression Eq. (5). Only Eq. (5) provides an accurate fit, with $\alpha=0.75$ and $\epsilon_0=32\text{meV}$.

We have measured the thermoelectric power of $\text{Bi}_2\text{Sr}_2\text{CaCu}_2\text{O}_8$ single crystals in the a-b plane. Fig. 11 shows the TEP from room temperature to 50K. The rather unusual temperature dependence is very similar to that observed for the a-b plane of $\text{YBa}_2\text{Cu}_3\text{O}_7$. For $\text{Bi}_2\text{Sr}_2\text{CaCu}_2\text{O}_8$ the TEP is always positive above T_c , suggesting in the simplest interpretation positive charge carriers.

3.2 Tunneling Measurements

We have investigated the superconducting state in $\text{Bi}_2\text{Sr}_2\text{CaCu}_2\text{O}_8$ and $\text{Bi}_0.1\text{Sr}_2.2\text{Ca}_{1.1}\text{Cu}_6.5\text{O}_y$ single crystals by break junction tunneling measurements [15]. Both SIS and Josephson tunneling are observed. The break junctions are formed and the measurements are carried out at 4.2K. Fig. 12a shows typical and reproducible Josephson tunneling for $\text{Bi}_2\text{Sr}_2\text{CaCu}_2\text{O}_8$. From this plot we estimate an energy gap $2\Delta_0/e = 45\text{mV}$, which leads to $2\Delta_0 = 5.9\text{K}T_c$. Similar values are extracted from SIS tunneling in the same material. This value corresponds to the gap in the a-b plane direction. Under certain conditions we find reproducible peak structure in dV/dI plots at regular voltage bias intervals, similar to that observed previously [17] in $\text{YBa}_2\text{Cu}_3\text{O}_7$ point contact tunnel junctions and interpreted in terms of the coulomb staircase.

We have also explored tunneling along the c-axis in $\text{Bi}_0.1\text{Sr}_2.2\text{Ca}_{1.1}\text{Cu}_6.5\text{O}_y$ single crystal needles. This is shown in Fig. 12b, where the dV/dI characteristics indicate an energy gap at $2\Delta_0/e = 37\text{mV}$, or $2\Delta_0 = 4.8\text{K}T_c$. This is the gap in the c-axis direction for this material.

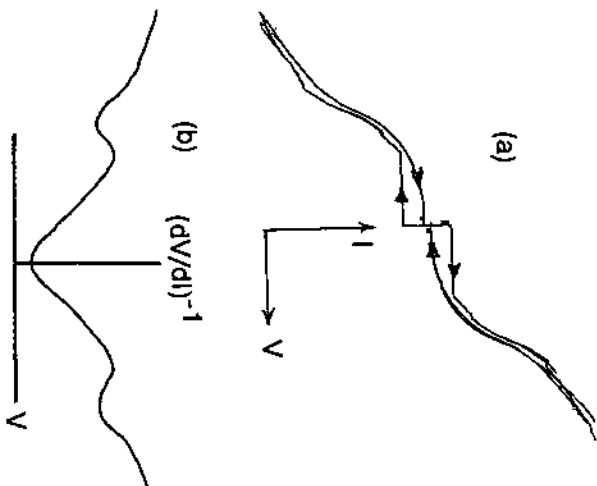


Figure 12. a) I-V characteristics of $\text{Bi}_2\text{Sr}_2\text{CaCu}_2\text{O}_8$ break junction, a-b plane, at 4.2K. Josephson tunneling is observed. b) dI/dV characteristics of $\text{Bi}_0.1\text{Sr}_2.2\text{Ca}_{1.1}\text{Cu}_6.5\text{O}_y$ break junction, c-axis, at 4.2K.

4. CONCLUSION

The normal state transport properties of Y-based and Bi-based superconducting oxides are unusual and suggestive of non-band transport mechanisms. The superconductivity does not appear to be confined to the copper-oxygen planes, and hence cannot be considered a strictly two dimensional effect. However, we expect the large anisotropy in the normal state to be reflected in anisotropic gap structure in the superconducting state. Reliable tunneling measurements in various crystal directions may resolve this interesting question.

We thank the following individuals for helpful interactions: T.W. Barbee III, L.C. Bourne, M.L. Cohen, C. Kim, and A. Iju. The x-ray analysis of the needle crystals was kindly provided by A. Zalkin. This research was supported in part by NSF grants DMR 83-51678 and DMR 84-00041, and by the Director, Office of Energy Research, Office of Basic Energy Sciences, Materials Sciences Division of the U.S. Department of Energy under contract No. DE-AC03-76SF00098. S. Hoen acknowledges support from the Fannie and John Hertz Foundation.

1. S.W. Tozer, A.W. Kleinsasser, T. Penny, D. Kaiser, and F. Holtzberg, *Phys. Rev. Lett.* **52**, 1768 (1987)
2. M.F. Crommie, A. Zettl, T.W. Barbee III, and M.L. Cohen, *Phys. Rev. B37*, 9734 (1988)
3. A.J. Heeger, in *Highly Conducting One Dimensional Solids*, ed. I.T. Devreese (Plenum, New York, 1979) p. 79
4. P.W. Anderson and Z. Zou, *Phys. Rev. Lett.* **60**, 132 (1988)
5. S.J. Hagen, T.W. Jing, Z.Z. Wang, J. Horvath, and N.P. Ong, *Phys. Rev. B37*, 7928 (1988)
6. M.F. Crommie, A.Y. Liu, A. Zettl, M.L. Cohen, P. Parilla, M.F. Hundley, W.N. Creager, S. Hoen, and M.S. Sherwin, (to be published)
7. P.B. Allen, W.E. Pickett, and H. Krakauer, *Phys. Rev. B37*, 7482 (1988)
8. L.R. Testardi, W.G. Moulton, H. Mathias, H.K. Ng, and C.M. Rey, *Phys. Rev. B37*, 2324 (1988)
9. D.W. Reagor, A. Migliori, Z. Fisk, R.D. Taylor, V. Kotsubo, K.A. Martin, and R.R. Ryan, (preprint)
10. J. Labbe and J. Bok, *Europhys. Lett.* **3**, 1225 (1987); V.Z. Kresin, *Phys. Rev. B35*, 8716 (1987)
11. G. Soda, D. Jerome, M. Weger, S. Alozon, J. Gallice, H. Robert, J.M. Fabre, and L. Giral, *J. Physique* **38**, 931 (1977)
12. S. Hoen, W.N. Creager, L.C. Bourne, M.F. Crommie, T.W. Barbee III, M.L. Cohen, A. Zettl, L. Bernardes, and J. Kinney, (to be published)
13. T.W. Barbee III, M.L. Cohen, L.C. Bourne, and A. Zettl, *J. Phys. C* (in press)
14. R.J. Cava, B. Barlogg, J.J. Krajewski, R. Farrow, L.W. Rupp Jr., A.E. White, K. Short, W.F. Peck, and T. Komecani, *Nature* **332**, 814 (1988)
15. P. Pinsukanjana, M.F. Crommie, S. Hoen, and A. Zettl (to be published)
16. G. Briceño, A. Behrooz, and A. Zettl (to be published)
17. P.J.M. van Bentum, R.T.M. Smokers, and H. van Kempen, *Phys. Rev. Lett.* **60**, 2543 (1988)

Transport Studies on High T_c Oxides

Y Iye

The Institute for Solid State Physics, The University of Tokyo,
Koyonggi, Miato-ku, Tokyo 106, Japan

1. INTRODUCTION

Despite the enormous increase of our knowledge due to the recent worldwide enthusiasm for high T_c research[1], it is fair to say that we understand remarkably poorly the physics underlying the remarkable phenomenon. One of the morris clearly emerged from the efforts is that we really have to accumulate reliable data and know the normal state electronic structures before talking about the mechanism of the high T_c . We have witnessed many cases in which what appeared to be key experimental results, on which a certain class of theoretical models put their bases, were seriously questioned by more careful later studies. In this paper we present some of our recent experimental results on the transport properties of the high T_c copper oxides and related materials. Topics to be covered are (1) anisotropic superconducting and normal transport properties of single crystal $YBa_2Cu_3O_{7-\delta}$, (2) metal-insulator transition, superconductivity and magnetism in $Bi_2Sr_2Ca_{1-x}Y_xCu_2O_{8+y}$, and (3) transport studies on some high T_c related cuprate materials.

2. ANISOTROPIC NORMAL TRANSPORT PROPERTIES OF $YBa_2Cu_3O_{7-\delta}$

Early experiments on high T_c materials were exclusively done on sintered polycrystalline samples. As a result of intensive effort towards improvement of crystal growth technique, increasing number of experimental data on single crystals became available. An empirical rule, which emerged from the studies of resistivity, Hall effect and thermoelectric power on single crystals, is that the transport coefficients measured in sintered polycrystalline samples basically reflect those in the basal plane of single crystals.

2.1 Resistivity

Tozer et al. [2] and Murata et al. [3], in their early work, reported quite unusual temperature dependences of anisotropic resistivity of $YBa_2Cu_3O_{7-\delta}$ single crystals. They found that while the ab-plane resistivity ρ_{ab} showed metallic T-linear behavior similar to the polycrystalline data, the c-axis resistivity was semiconductor-like. Anderson and Zou [4] fitted the ρ_{ab} data of Tozer et al. [2] to a functional form $\rho_c = AT + B/T$ and suggested that the intrinsic behavior of ρ_c would be $\sim 1/T$. The unusual temperature dependences of ρ_{ab} and $\rho_c \sim 1/T$, were claimed by Anderson and Zou [4] to be nearly explained in the holon-spinon transport scheme based on the resonating valence bond (RVB) model originally proposed by Anderson [5].

The scenario for the electrical transport in the RVB model is as follows: The charge carriers in the two-dimensional CuO_2 layer are holons. Holons are scattered by spinons, with scattering rate proportional to the number of thermally excited spinons, which is linear in T . This leads to $\rho_{ab} \sim T$. Transport along